Design and Implementation of Hybrid Techniques and DA-based Reconfigurable FIR Filter Design for Noise Removal in EEG Signals on FPGA

C. SRINIVASA MURTHY, K. SRIDEVI
GITAM Institute of Technology, GITAM Deemed to be University, Visakhapatnam, Andhrapradesh, INDIA

Abstract: - Virtual Reality (VR) technology assists physically challenged personnel in their daily routine activities. The evolution of technology has enhanced the critical activities of people who use wheelchairs by extracting features through electroencephalogram (EEG) and promoting options for their choice for decision-making on their own. During extraction of EEG, signal artifacts may mislead the decision-making environment. Hence noise has to be removed with help of an FIR filter for accuracy. In this context utilization of finite impulse response (FIR) filters are so vital hence filters are incorporated with the hidden Markov model (HMM) and Gaussian mixture model (GMM) and supervised machine learning architecture of multirate support vector machine (SVM). The proposed EEG-based diagnosis system is a fully automated audio announcement system. The entire environment has been developed by Verilog HDL and MATLAB. Validated on Artix-7 FPGA development board and synthesized with Vivado Design Suite 2018.1. Obtained results exhibit an enhancement of 32% of signal-to-noise ratio (SNR),7% of mean square error (MSE), and 69% of abnormality recognition.

Key-Words: - Virtual Reality (VR), electroencephalogram (EEG), hidden Markov model (HMM), Gaussian mixture model (GMM), support vector machine (SVM).

Received: June 29, 2021. Revised: May 14, 2022. Accepted: June 12, 2022. Published: July 14, 2022.

1 Introduction

Electroencephalogram (EEG) signals are the primary signals which can be used clinically to detect human brain activities. EEG signals might be corrupted by a motion of the lens during collecting data from electrode results artifacts. This may occur because of breathing and muscle contractions, as well as an imbalanced contact between the skin and the surface of the electrode [2-5]. Accidental noise signals, known as motion artifacts, can hurt EEG reading and make them unsuitable for analysis **[6**]. The elimination of motion artifacts from EEG signals is very necessary to determine the optimal EEG signal for monitoring and analysis of brain activities. Several alternative methods have been proposed to remove artifacts from recorded EEG signals. The most practical technique to eliminate motion artifacts is to treat the signal with a digital filter. Filters can eliminate extraneous signals without changing the original signal if the predetermined objective is used as a reference [8-11]. As a necessity, it is owned to demand exact reference signals. The removal of EEG motion artifacts is, however, inadequate. The Discrete Wavelet transform (DWT) [12] is one of the most widely utilized de-noising algorithms in applications. In earlier research Hashim [14] employed the wavelet threshold access to minimize motion artifact noise in EEG recordings. EEG signal baseline wander should be kept to a minimum. The zero-phase high pass FIR Equi-ripple filtering approach was suggested by Daqroud [8].

2 Related Work

In **[7]** passive wavelet transform has been employed to extract the motion of artifacts from EEG signals via non-contact capacitive coupling electrodes [13-15]. The discrete wavelet process is required to pick appropriate wavelet functions and thresholds, which renders the wavelet a non-adaptive approach. To address the wavelet transform's inadequacies in terms of flexibility alone [16-19], Huang proposed an empirical mode decomposition (EMD) procedure, which is an adaptive technique for decomposing signals into a limited number of intrinsic mode functions (IMFs). Blanco-Velasco proposed an EEG optimization strategy based on the EMD to reduce

high-frequency noise and baseline drift. Mode mixing, on either side, is a common issue in the EMD process that causes IMFs to be extracted inadequately. Discrete wavelet transformations have been advocated for quality removal in wavelet vectors. For recognition of transmission line short-circuit faults [20], the discrete wavelet transform has been employed in fault analysis, EEG de-noising, and disease recognition detection.

DWT is used to detect and eliminate movement artifacts in EEG signals. RTP and RTCP methods outperform the EMD method when a filter is employed to reduce power-line intrusion and accurate baseline drift. Hence we propose a method to remove motion artifacts from practical EEG recordings based on discrete wavelet transform and wavelet thresholding in this article. At this point in the process of validating the viability of the proposed algorithm, real-time EEG has been captured and reproduced signals. In terms of re-storage of the new EEG theta delta alpha-beta (TDAB) complexes and signal-to-noise ratio augmentation of EEG signals associated with the discrete wavelet transform and EMD motion artifact elimination have been effectively enhanced and the proposed technique executes much improved grades. The goal of the current effort is to advance artifact exclusion practice capable of identifying interference in EEG recordings in a variety of situations and frames. The proposed technique [18] includes a supplemental description for improved recognition and organization of abnormalities, as well as probable pulse-related disruptions. For artifact removal, extracting features, and detecting deviations the proposed strategy consists of a three-stage method for assembling raw EEG signals, transformed. The data has been classified using classifiers, and the results have been applied to FPGA for displaying the abnormal in the display unit to take a decision. The method improves the signal-to-noise ratio by gaining access to signals that can protect the unique quality waveform without corrupting the original raw data (SNR). The proposed method expands the system which can recover all the parameters available in an EEG raw signal. Several denoising methods have been proposed in the literature such as median filter, discrete cosine transform, and discrete wavelet transform. In [21] proposed multi-objective flower pollination algorithm (MOFPA) with wavelet transform (WT) for removal of artifacts and denoising of EEG signals and different parameters analysis are done in terms of SNR, PSNR, and MSE. In [22] is focused on Virtual reality for improving the signal quality by removing artifacts. Based on the results obtained, correction prediction is 83% and 77% improvement in SNR. At the onset, a filtering technique using a band-pass finite impulse response (FIR) filter with a frequency range of 0.5–40 Hz is used to remove various artifacts and sounds mixed with raw EEG signals. The DWT is then employed to evaluate the signals in the time-frequency domain because EEGs are highly non-linear and non-stationary signals in nature. For feature extraction, DWT with four-level decomposition is used with the db6 mother wavelet. To effectively categorize the signal, a new feature set formed of eleven non-linear statistical features collected from each sub-band resulting from wavelet decomposition is given to the input of an ANN. Finally, to increase classification performance, a unique approach called the sequential window algorithm is used. This study achieved 99.44 percent mean classification accuracy, 80.66 percent average sensitivity, 4.12-second mean latency, and 0.2 percent average false positive rate (FPR). This research successfully reduces latency time with greater accuracy and a lower FPR [23]. Different approaches for removing artifacts have been proposed, however, artifact removal research remains a work in progress. This paper focuses on the current state of contaminated artifact removal. First, we'll go through the features of EEG data and the many sorts of artifacts. Following that, a basic overview of current state-of-the-art procedures is offered, as well as a detailed study of them. Finally, a comparison analysis is presented to aid in the selection of appropriate approaches for a given application [24]. Several novel methods for analyzing brain bioelectrical signals were demonstrated and compared. It also covers both traditional and modern methods for removing noise contamination, such as digital adaptive and non-adaptive filtering, signal decomposition methods based on blind source separation, and wavelet transformation [25]. It distinguishes sleep stages and extracts novel information from the sleep EEG to aid clinicians in the diagnosis and treatment of sleep disorders. This theory is based on exclusive EEG datasets from Physionet, as well as the MIT-BIH, which is received and reported by scientists for sleep range analysis and prognosis. ML-based classifier utilizing Ensemble Bagged Tree classifier achieved detection

accuracy of 95.9% on 18 records with 10197 epochs, according to results [26].

Background: The EEG signals are a mix of small amplitude in μV and different artifacts which are contaminated due to the lens during the recording of the signals, all these facts affect a change of signal properties and these changes will create major issues while analysing and diagnosing the abnormalities. The EEG signals are also affected due to power line noise, if signals frequency is above 45 Hz and it makes it difficult to retrieve original information and creates problems in effective diagnosis. In this research work, the FIR filter plays a major role in removing artifacts and creating noiseless signals for proper further diagnosis. The EEG signals are collected from https://physionet.org/news/post/397 and this database has a sampling rate of 256 with a period of 5 seconds. The second process involved in the FIR filter is an adjustment of DC shift and removal of it by calculating the mean and setting it to ground level. After the successful removal of artifacts in EEG signals, different parameters like SNR, MSE, and PNSR are analysed and compared with existing works.

Motivation: In this work, the subjected EEG signals are divided into different windows and each window has 512 samples and applied to FIR filter design and its performance analysis is carried out. For the effective removal of artifacts, 64 tap FIR filter is designed with the help fast RNS-based multiplier. To minimize latency created by partial products, Parallel Prefix Adder (PPA) is used along with the proposed multiplier, the overall design is high throughput and low latency. The digital FIR filter with 64^{th} order is subjected to epochs of each signal and analysis has been done through different metrics to measure the removal of noises and to retain signals quality. The 64-tap FIR filter uses Kaiser Window with low pass filter response and based on metrics analysis, it is found that the proposed design is better than existing works.

Objectives: Design of efficient FIR filter for effective removal of artifacts that are contaminated through many sources such as 45Hx noise, eye blink, EMG noise, and many more, but the noise which is affected by power line of frequency of 45Hz is dominated by noise and removal the of it, is a major concern. Therefore, removal of such noises is a major motivation of this work, and filter signals should ready proper diagnosis and good quality with high accuracy. Based on a literature survey done on various techniques used for the removal of artifacts, the following objectives are highlighted for this research work.

1.Detailed study on different properties and characteristics in EEG signals

2.Detailed analysis of FIR filter design for optimization of power consumption, latency, and improvement in throughput.

3.Design of FIR with both Kaiser Window and low pass filter in Xilinx Design suite software using Verilog HDL and generation of coefficients with help FDA tool in MATLAB.

Detailed analysis of results obtained through proposed FIR filter and comparison between proposed and existing in terms of parameter metrics.

About EEG Databases: The two strategies for eliminating raw EEG signals are simulated databases and real-time databases. The standard database contains a selection of EEG signal events of comparable length, which is provided with the dataset from the MIT-BIH Noise Stress Test Database for duplication commitments. A distinct signal includes time-shifting TDAB morphology in a pair of regular and irregular EEG pulses and based on the pair and irregular pulse, the abnormal is detected.

3 Proposed Automatic Abnormality Detection System for Physically Challenged Peoples

EEG files have been created by adding motion distortions to EEG data outputs at various levels of signal-to-noise ratio. In hospitals, EEG signal acquisition systems are typically large and maintain excellent precision and long-term monitoring. All types of EEG recording equipment, from single-lead to 12-lead, are available. In real-time monitoring of a patient's condition through the use of many sensors' certain wearable health-monitoring technologies improve awareness on either side. The dataset collecting stage of EEG includes the collection of sensor forms, the position of sensors to point, the number of sensors, and the hardware required for data acquisition, archiving, and dissemination. In a few real-time EEG detecting techniques, continuous EEG sensor acquisition may be employed. It is a difficult task to target EEG signals to multiple feature assessments such as quality, reliability, and punctuality. The erroneous disease identification and a major impact on clinical outcomes will result from

the corrupted collected data. Fig.1 shows the proposed overall architecture of abnormalities detection and its classification which is based on SVM and architecture consisting of an FIR filter, Block memory generator and its controller, feature extraction using HMM and GMM, and an SVM-based classifier. The sample of EEG signal captured by wireless Neurosky Mind wave Mobile 2 device is stored in block memory which is off-chip BRAM. The stored sample values are applied to the FIR filter to eliminate noise samples that have high-frequency signals and the filter uses fixed-point arithmetic operations of size 16 bits including sign bit. The block random access memory (BRAM) controller is an IP core industry-standard component instantiation in the top-level design which communicates between overall system design and memory. The raw sample of EEG signals is processed through an FIR filter and then applied to HMM and GMM to extract abnormal features present in the filtered signals. For each extracted feature, the variances, energy, and meaningful metrics are calculated and these metrics are used for classifications. The multi-rate SVM which uses the sigmoid function, has two phases such as learning (training) and testing, in the first phase, training the network against normal and abnormal signals, and second, the phase is testing to detect abnormal in the selected EEG signal from data sets and measurement accuracy and based on obtained metrics, the SVM classifies the dataset into normal and abnormal. For the implementation of HMM, GMM, and SVM functionality, double-precision floating point-based multipliers and adders are used in the proposed system. The main advantage of floating-point operations compared to fixed-point operation is that distortions are almost zero in floating-point operations therefore detection of abnormalities are accurate. In floating-point operations format has 52 bits for mantissa, 11bits exponent, and 1 bit for the sign. For validation of floating operations results that are obtained in digital software tools compared with MATLAB results since MATLAB tool works on based floating-point and it is found that both results are same.

4 Feature Extraction using HMM and GMM Modules

In this paper, GMM with HMM is applied to filtered EEG signals for extraction of features and classifications of different categories. HMM, mathematical theory models are provided to understand the use of HMM as shown in Fig.2. For abnormal features extraction in EEG signals through HMM and GMM have been pipelined in this work and each element of HMM has been made mandatory for proper identification of disorders. Characteristics of HMM are as follows. The number of states in HMM is N and it has its physical significance and acts a as hidden part of Baki's model allowing transitions to each state which has modeled the index compato red the present state [10]. The number of observations (M) is distinct from other observations and these are the output of the modeled system and all states are represented as S=$\{S1, S2, S3, \ldots\ldots Sn\}$.

- The distribution of probability in each transition state is X= $\{x_{ij}\}$which provides the probability of states reaching to final decision from any other states and it is given by.

$$x_{ij} = A\left[y_{t+1} = B_j | y_t = B_i\right], 1 \leq i, j \geq N$$

For lower indexing then present state, the $x_{ij} = 0$ which has transitions to any other states.

- P is probability distribution of symbol which is observed in j states i.e $P = p_j(k)$, where $p_j(k) = A\left[U_k x_{ij} \middle| y_t = B_j\right], 1 \leq j \leq N \; and \; 1 \leq k \leq M$
- S_i is initial state distribution and it is given by $S_i = A[x_1 = B_j]$, therefore the complete features extractions required two level decomposition model parameters such as N , M to measure the constants A,B, P and S_i, the complete HMM function is given by Q=(A,B,S_i).

The features extraction using HMM and its selection to get trained samples as shown in Fig.2. **Observations (M):** The proposed system employs numerous sequences to collect enough samples of data to establish efficient model that will estimate distinct samples from other samples. In GMM the number of mixtures in each state (M) the distributions in Gaussian for different weights will form a new density probability which will be generated by HMM. According to the fundamental concept, a higher value of M would allow for accurate signals modelling, because of very short duration of other signals. A larger M value would leave very few estimates for these signals. As a result, accuracy in signal estimation occurs for M = 4 may produce better categorization results into normal and abnormal shown in Fig.2.

The number of iterations and Convergence: The two existing criteria in HMM are used for training to convergence and the number of iterations. HMMs are trained by raising the model's based on score for EEG signals collection of observation samples.

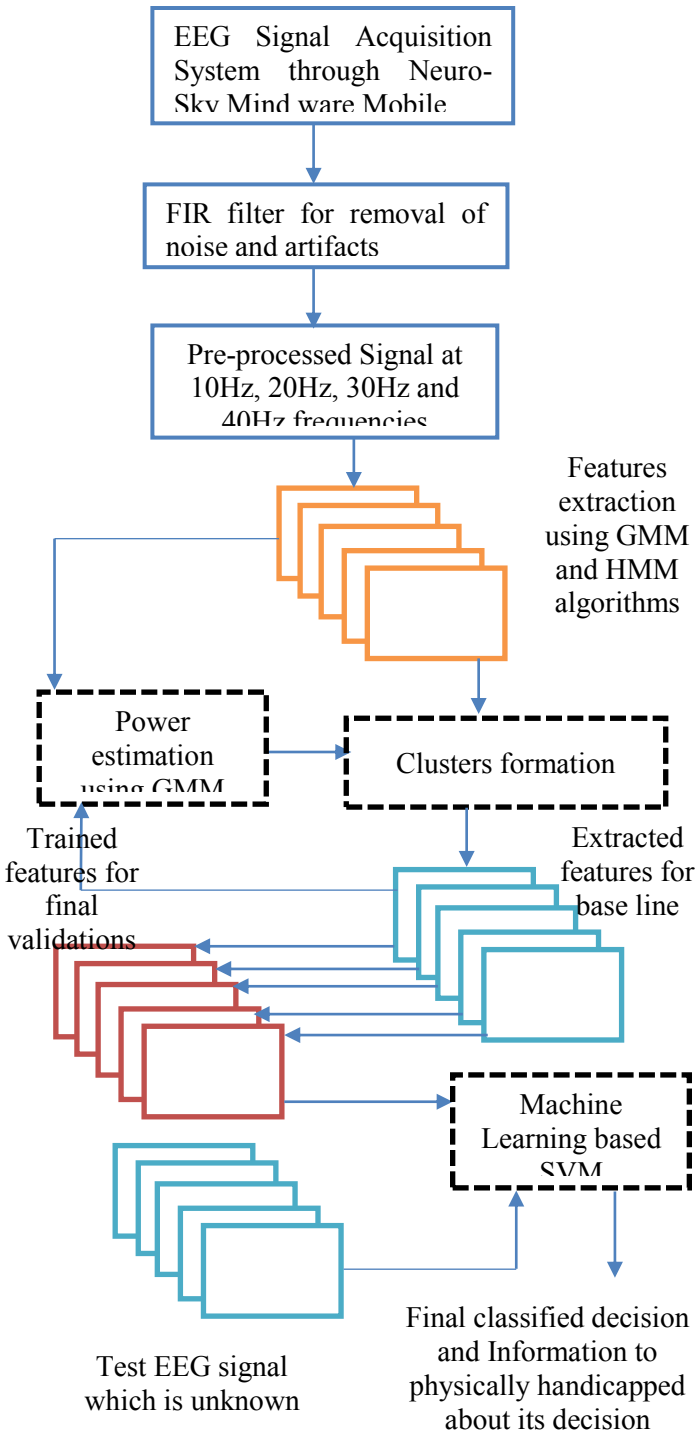

Fig. 1: Proposed diagram of FIR filter for artifact removal and abnormal detection using SVM

The accurate and tolerance level, which is set to 0.0001, refers to the percentage increase in this score from the previous iteration, r model to be regarded to have converged if the gain in score for the current iteration is less than 0.0001. In general the HMMs required 35-51 iterations to converge, however this depends on a variety of criteria, including tolerance, data, and good modelling parameter selection. The 80 iterations are a mandatory number having one of these two conditions is met, the training comes for final decision. Median filtering (MF) is used along with FIR which is windows based model (w) can replace the intermediate signals for optimization has been applied for filtering the noise at very low frequency signals to produce nonlinear smooth signals. The prescribed series of n samples within a window of length L as per equation (1), where M is the median value.

$$W = \{x_n\},\ -L \le i \le L \qquad (1)$$
$$\text{where } M = median\ (x_n)$$

In the VLSI environment effectiveness has to be planned in terms of look up tables (LUTs) and slice register (SR) for less consumption of hardware resources**.** Hence a combination of DCT and FIR filters has been employed for efficient filtrations at both low and higher. The phases of EEG de-noising based on MF can be summarized as follows: A median filter with a width of 200 ms is used to separate the TDAB complexes and P waves from the noisy EEG input. A 600-ms MF is used to separate T waves from the following signal. The second filter action restricts the baseline of the EEG signal, which has to be subtracted from the noisy EEG data to obtain the adjusted baseline EEG signal. The basic FIR filter function is given by

$$y(z) = \sum_{j=0}^{M-1} x(j)h^{-j} = \sum_{j=0}^{M-1} x(n)h(n-k) \qquad (2)$$

Where **k** is the length of the filter, in this design, the k is 0 to 63 [21]. Equation (2) proposes FIR filter operation with the direct structure which requires less number of registers and its internal architecture is shown in Fig.3. The Conventional FIR filter design uses a binary number system for adders and multipliers, which results in increased propagation and net delays and limits the pace of operations. To overcome these drawbacks, the suggested RNS-based FIR filter presented in equation (1) employs a faster modified Parallel Prefix Adder (PPA) that avoids carry bit propagation The results of the existing PPA

and modified PPA are displayed in Table 1. Once the power band performance from the EEG signals have been extracted, computation of incident-linked (de)synchronization (ERD/ERS) directory, a measure of band power shift in EEG is carried out which has first introduced by Pfurtscheller as well as Aranibar [34] and can be determined as follows:

$$\frac{ERD}{ERS}\% = \frac{Baseline\ IBP - Test\ IBP}{Base\ line\ IBP} x100$$

Where IBP is Interval band power is.

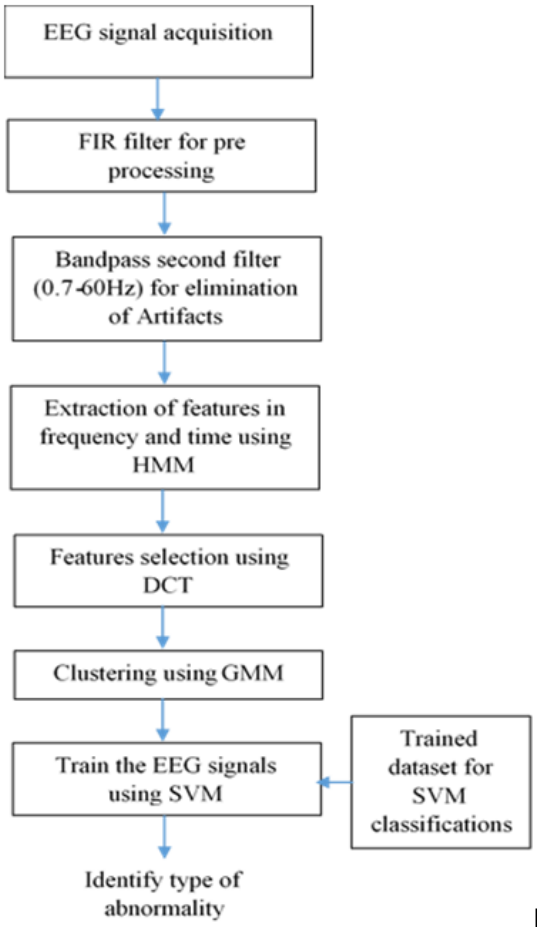

Fig. 2: Proposed abnormalities identification and features extraction using HMM and SVM based Classifications.

4.1 DCT Transform

The discrete cosine transform (DCT) is employed for signal transmission as well as used for the presentation of a digital image processing technique that converts the time-domain function to a frequency domain function. The Discrete Cosine Transform is the true part of the Discrete Fourier Transform of a signal w (k) represented in equation (3).

$$y(k) = w(k)\sum_{n=1}^{N} \mathrm{x(n)}\cos\left(\frac{\pi(2n-1)(-1)}{2N}\right) \quad (3)$$

Here the length of the noisy EEG signal is represented by N as well as DCT quantities is represented by $w(k)$ which is computed as follows:

$$w(k) = \begin{cases} \frac{1}{\sqrt{N}} & if\ k = 1 \\ \sqrt{\frac{2}{N}} & if\ 2 \le k \le N \end{cases}$$

Substitute k as well as n in the y (k) equation to determine their inverse form. The DCT provides excellent energy density in the case of highly interlinked data. Once the energy compression feature of DCT is obtained then this feature is conversed and provided with information to various predefined EEG signals operations. Further, we found that the DCT spectrum is situated at a low frequency, which represents the initial characteristics of the DCT transform. The very first coefficients that are generated using a one-dimensional DCT transform are assumed to correlate with BW artifacts in the EEG signal. In input EEG signals, correlated data is extracted by DCT and calculated their energy through transform coefficients.

5 Classification using Multi-Rate SVM

To categorize data into normal as well as abnormal classifications, a precise classifier based on Neural Networks using SVM classifiers can be employed. Machine learning is a type of artificial intelligence (AI) that enables computers to analyze the records of an individual with trained algorithms, and also it can be used to pre-process systems with various datasets, and finally, it recognizes each record separately. The technique of machine learning is to saturate the data to identify probable patterns in the data as well as to modify program actions. The technique of Machine learning includes unsupervised as well as supervised learning. Preparation of information in targeted learning exists in the form (Xn,Yn)n = 1,2,.... N, with Xn representing examples from an input space X as well as Yn is generated by an undefined and unpredictable process with input as Xn. The most common technical issue faced in supervised learning is classification as well as regression. On the other hand, unsupervised Learning is provided with a set of samples Xn, n = 1,2,.... N, however, the labels Yn are

unstable. Although Yn is not accessible, the outcomes that seem to be available are referred to as unsupervised learning. In this scenario, learning problems include an increase in data clusters; the center of clusters, as well as the clusters themselves of the input data is often associated with pattern classifications as well as structure evaluations. We propose the Support Vector Machine (SVM) as a machine learning algorithm that can provide better results while separating datasets and have a more stable presentation when dealing with data uncertainty in our technique. The datasets that were initially generated were stored in separate training and testing sets that were independent of each other, finally through VLSI programming, the SVM algorithm was applied to the data pre-processing. With the help of clustering, the excluded structures are then linked to the training data set structure. Cross-justification is often used to estimate how a machine learning algorithm will operate when confronted with unexpected input. The Machine learning algorithms generate a hypothesis and thereafter evaluate it using the same data. During K-fold cross-authentication, the data is unevenly divided into K divisions. To train the sets residual data sets are used and one more data is used for analysis and be evaluated, every division set should be dignified K times. To test the viability of the technique proposed, Three-fold cross-validation is employed. Every row is a tradeoff to check the accuracy using a classifier. Although the classifiers are mongrelized, the classification accuracy gained from them is described as the load.

6 Performance Analysis in Terms of Accuracy, FER and FAR

Some of the parameters that can be employed to measure the efficiency of the projected procedures include theta, delta, alpha, and beta (TDAB) values which have to be identified for accurate calculation of SNR, accuracy, as well as error rate. Classifier evaluation metrics areas followed. Three essential analytical procedures are measured to identify the classification performance of the proposed method. We compute the accuracy of the algorithm classifications as the fraction of all true classifications of overall classifications as seen in Fig.2.Initially, limit the algorithm's classification for accuracy calculation to a fraction of all true classifications throughout all classifications.

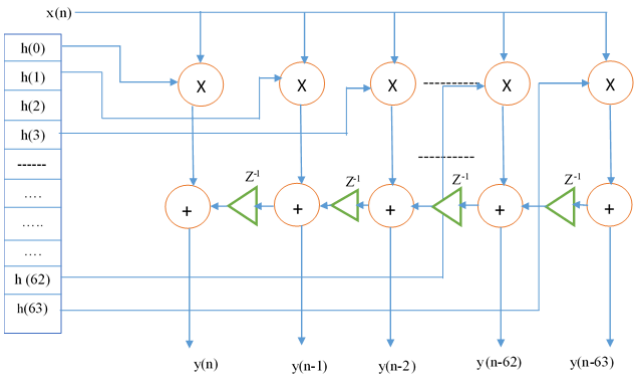

Fig. 3: Internal Architecture of FIR filter with64 taps [21]

$$\text{Accuracy} = \frac{\Sigma(\text{TP}+\text{TN})}{\Sigma(TP+TN+FP+FN)}$$

Where TP is true positive, TN is true negative, FP is false positive and FN is false negative.

Furthermore, the classification of the algorithms for false error rate (FER) has been computed as the ratio of falsely classified as per the equation below:

$$\text{FER} = \frac{\Sigma(\text{FN})}{\Sigma(TN+FN)}$$

Finally, the classification algorithm's sensitivity is computed and is represented as follows:

$$\text{s} = \frac{\text{TN}-\text{FAR}}{(1-FAR)}$$

Here the hit rate and false acceptance rate is represented by HR and FAR respectively and is given as follows:

$$\text{HR} = \frac{\Sigma(\text{TP})}{\Sigma(TP+FN)}$$

$$\text{FAR} = \frac{\Sigma(\text{FP})}{\Sigma(FP+TN)}$$

The efficiencies and FAR are 1 and 0 respectively only when the classifications are correct. Precision, FAR, as well as s, are all computed separately.

7 Results and Discussion

There is a significant improvement in the detection of abnormalities as compared to conventional classifiers, as evidenced by performance indicators like accuracy, SNR, PSNR, and Energy. This is due to the fact that there are more samples available in the given data set for training the HMMs, and the processing time is more, in order to minimize the elapsed time, GMM has been used to train the

network and stored in memory and then applied to HMM. Furthermore, because each and every sequence length is longer, hence DCT model provides a superior fit for describing non-disease and illness data. Hybrid types of HMMs, in which multilayer perceptions or clustering algorithms are utilized to obtain non-disease data, can be employed to create better models. As the number of data samples increases and the number of training samples grows, we can see that performance improves in obtained results shown in Table 4. The next stage is real-time validation in EEG data samples that are present in the database after designing the detector and classifier HMMs. At this stage, no more data processing or feature extraction is required. This is profit accomplished using the HMMs from the previous existing works. The validation method for the performance of the HMM-based detection and classification system and its accuracy is depicted in Figure 7. For a few signals with definite uncertainty, signal are considered in order to prove the functionality of HMM system and this allows us to compare abnormalities detection and their performance to the diagnosis. Tables 3 and 4 exhibits the utilization of resources by the proposed system for effective detection of abnormalities and hardware resources utilized are generated through the synthesis process. Table 3 shows PSNR and SNR values for different activities. The proposed HMM has been used as the main model for feature extraction and SVM classification for the detection of abnormality based on trained features derived from the entire dataset. In abnormal detection, much work has been carried out with cascading HMMs such as HMM1, HMM2 and HMM3 or using other classifiers like MLP. The proposed hybrid method based on HMM, GMM, and SVM provides better accuracy and randomized parameters like PNSR and SNR. This strategy has potentially provided well precise outcomes. In addition, in the existing works the sampling frequency employed varies by location of abnormality due to more artifacts. Different EEG monitors are accompanied by different power supplies (amplitude in V), which can be adjusted according to the expert's preferences. These quantities may influence the extracted features and have been standardized in the industry as well in research. More trustworthy features can be extracted with a better specification of the exact shape, length, and other parameters of the EEG spike. In addition, a uniform database for all EEGs would be extremely useful in comparing and contrasting all of these methods and features. Expert-provided signal exemplars would also be very useful for the Non-disease data. It is necessary to provide an example dataset with signals or artifacts that are identified by experts as being very similar to existing. Models trained on such exemplars would very certainly be producing superior results. All of the reported datasets are associated with various anomalies, as described below, in Table 1. Each dataset comprises 3600 samples, which are rehabilitated to binary using MATLAB source code and stored in the FPGA's block-RAM (BRAM). When compared to previous works, all projected practices for precise irregularity recognition can generate performance with 99% exactness and there is a development of 5%in accuracy and detection of abnormalities. Table 2 shows in positions of anomaly recognition and recognition precision in percentage, the projected effort, and the present effort are equated. The projected automated abnormality recognition system is originated to be proficient in noticing anomalies from the consistent database, which are from the MIT-BIH arrhythmia database the suggested and validated by medical export and proposed results shown in Table 1 and Table2, based on obtained results the Atrial fibrillation with 99% accuracy, Atrial flutter with 68.2% accuracy, Normal Sinus rhythm with 93% accuracy, Sinus Tachycardia with 65 percent accuracy, and Ventricular Fibrillation with 100% precision, among other diseases are shown in Table 2. The projected scheme has a precision of 85.24 percent on average as shown in Fig.4 and SSIM is shown in Fig.3 (b) and PSNR is shown in Fig.4(a).

Table 1. Number of records present in the database for various abnormalities

Database record	Name of the abnormalities	Database count
2-14	Activity:1(More Reading)	14
2-17	Activity:2(Peak-Peak variations)	17
2-11	Activity:3(Eyes movement)	11
2-14	Activity:4(Left Leg movement)	14
2-15	Activity:5(Right Leg movement)	15

DCT has excellent energy compression and power indulgence abilities compared to STFT, FF, and the Fig. 8(b) shows the EEG database record no.15 of atrial fibrillation and 12 of atrial flutter, and their energy compaction results shown in Fig. 8(c) through lettering Verilog HDL programming language and manufactured by VIVADO design suite 2018.**1.** The RTL design diagram is shown in Fig.9, the simulated results are shown in Fig.9the simulated results of artifacts deletion and types removed results are shown in Fig.8 and 9the manufactured effects of the projected health observing scheme are shown in Table. 4. Since the device is quick and has been tested against a standard database, the prototype module established will undoubtedly aid in the monitoring of patients' health. The outcomes showed that the system operates at 113.148MHz, power consumption is of 0.082Watts, several LUTs utilized is 485, area (no of slice register) is 284 and delay is 4.419ns. The proposed system is synthesized in Xilinx software tool and final results are interface with microcontroller (Arduino Uno board), from it, the GSM is an interface to send a message about soldier's health situations to medical professionals or concerned persons so that soldiers life can be saved instantly. The entire system is designed in Verilog HDL and processed through FPAG design flow like synthesis, mapping, translation, place & route, and finally bit steam file is generated and the same file is configured on FPGA. Based synthesis report, the total delay of the proposed system is 2.5ns and power consumption is 1.8mW.

Table 2. Comparative analysis of proposed research work with existing work in terms of detection of different abnormalities and accuracy

Database record number	Name of the abnormality	Detected (YES/NO)	Proposed work Accuracy	Existing work Accuracy
1		Yes		
2		Yes		
3		Yes		
4		Yes		
5		Yes		
6		Yes	98%	92.2%
7	Activity:1	Yes		
8		Yes		
9		Yes		
10		Yes		
11		Yes		
12		Yes		
1		Yes		
2		Yes		
3		No		
4		Yes		
5		Yes		
6		No		
7		Yes	81%	78.2%
8	Activity:2	No		
9		Yes		
10		No		
11		Yes		
12		Yes		
13		No		
14		Yes		
15		Yes		
16		No		
17		Yes		
18		Yes		
1		Yes		
2		Yes		
3		Yes		
4	Activity:3	Yes		
5		Yes		
6		Yes		
7		Yes		
8		Yes		
9		Yes		
10		Yes	89%	79%
11		Yes		
12		Yes		
13		No		
14		Yes		
15		Yes		
16		Yes		

1 2 3 4 5 6 7 8 9 10 11 12 13 14 15	Activity:4	No Yes Yes Yes No No No Yes Yes Yes Yes Yes Yes No No	76%	69%
1 2 3 4 5 6 7 8 9 10 11 12	Activity:5	Yes Yes Yes Yes Yes Yes Yes Yes Yes Yes Yes Yes	100%	89.7%

All pulse detecting algorithms functioned perfectly for a large number of data present in the MIT-BIH Arrhythmia Database. However, because of the irregular heartbeat as well as interference effect, only a few records in this database possessed dynamic signals, especially 12, 18, 16, 15, 12 records. Earlier, these records were utilized to examine the noise tolerance of earlier investigations. As per the Physio Net web-based resource, the signal from record 73 seems to be more challenging in MIT-BIH Arrhythmia Database because of the signal's characteristic pattern with uneven beats. Table 1 compares the algorithm's output for another few challenging records such as 12, 18, 16, 15, and 12. The heartbeat indicator can fluctuate between normal and abnormal beat signals as evidenced by records 12, 18, 16, 15, and 12. The signal from records 20 and 73 revealed a regular, varied heartbeat, and a normal, atrial late, premature ventricular contraction beat respectively. As seen in Fig.9, the EEG signal for record 53 is a composite of regular as well as controlled ventricular reduction beats. To remove the artifact outcome, pre-processing is very important for EEG signals. The proposed technique for removing artifacts from raw EEG data uses a median filter, HMM, GMM, as well as DCT with the height constants of the DCT component set. SVM classifiers have been used to distinguish correct datasets as output. Furthermore, the output signal has been given as input to RTP as well as RTCP before being saved in loading procedures. The proposed algorithm is more functional and provides enhanced performance. In the database, there are 100 EEG signals taken from the Physio net website, out of 100 EEG databases, we have considered 10 EEG signals due to the limitation of internal memory the of FPGA hardware board.

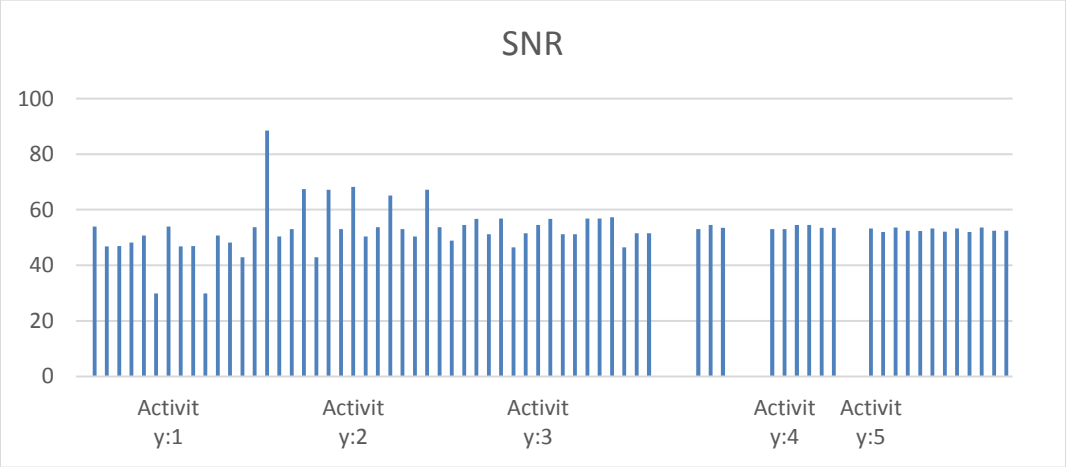

Fig. 4: Average SNR of each activity for different abnormalities

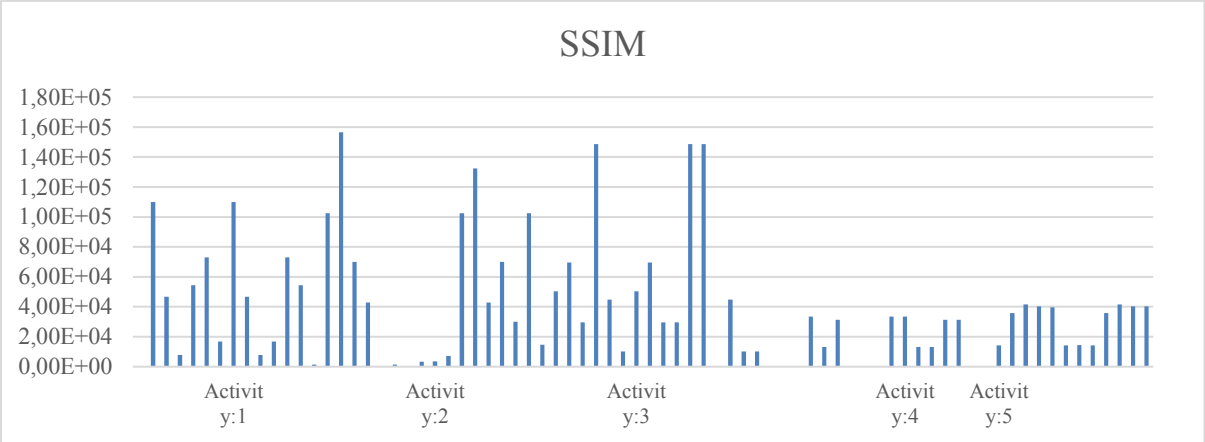

Fig. 5: Average SSIM of each activity for different abnormalities

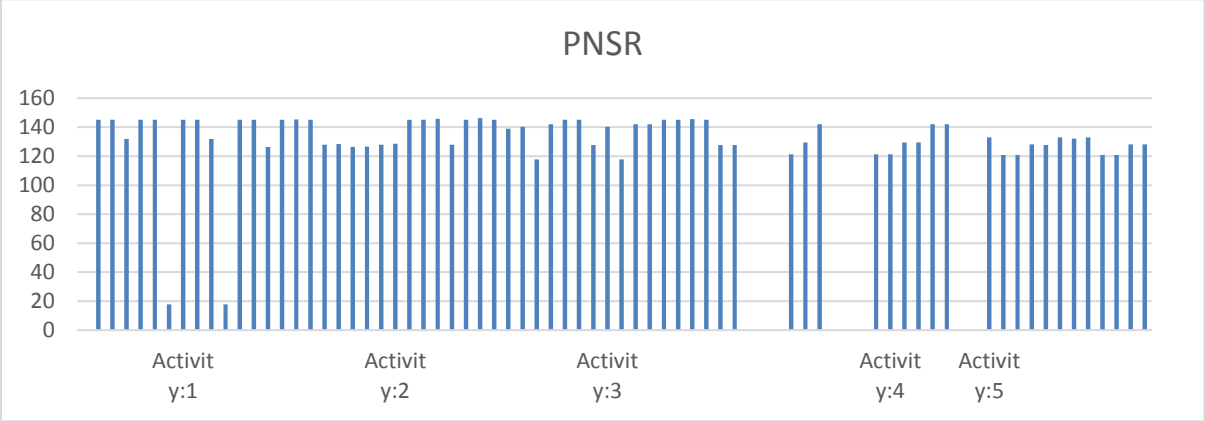

Fig. 6: Average PSNR of each activity for different abnormalities

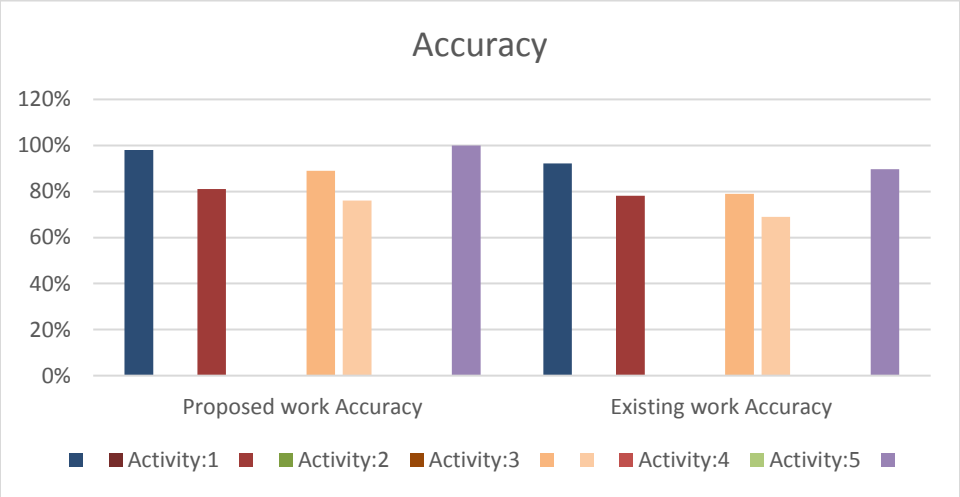

Fig. 7: Average accuracy of all types of abnormalities and their corresponding activities

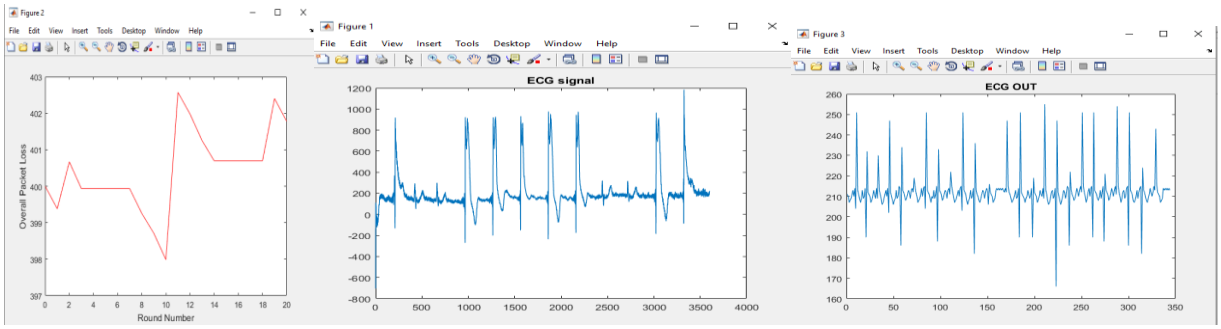

(a) (b) (c)

Fig. 8: Database EEG signals, (a) packet loss w.r.t number of round to upload the packet into cloud for storage (c) After removal of artifacts in MATLAB.

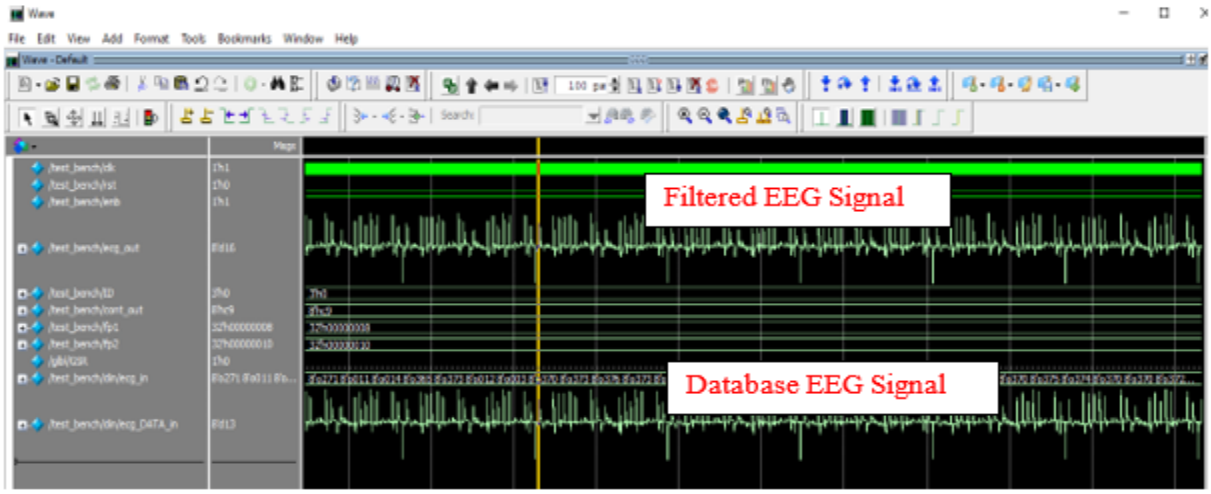

Fig. 9: Artifacts removed simulated results of EEG signals for automatic detection of abnormality

Database record number	Name of the abnormality	Detected (YES/NO)	SNR	SSIM	PNSR
1		Yes	53.96	1.0986e+05	145.0401
2		Yes	46.84	4.6745e+04	145.0402
3		Yes	46.92	7.8190e+03	131.9772
4		Yes	48.2324	5.4343e+04	145.0401
5		Yes	50.7312	7.2932e+04	145.0682
6		Yes	29.9189	1.6889e+04	17.7023
7	Activity:1	Yes	53.9620	1.0986e+05	145.0401
8		Yes	46.8485	4.6745e+04	145.0402
9		Yes	46.9271	7.8190e+03	131.9772
10		Yes	29.9198	1.6889e+04	17.7023
11		Yes	50.7312	7.2932e+04	145.0682
12		Yes	48.2324	5.4347e+04	145.0401
1		Yes	42.8603	1.4563e+03	126.3978
2		Yes	53.6969	1.0246e+05	145.0476
3		No	88.5	1.5646e+05	145.4576
4		Yes	50.3966	7.0063e+04	145.0401
5		Yes	53.0835	4.2881e+04	127.9498
6		No	67.45	84.5	128.34
7		Yes	42.8603	1.4563e+03	126.3978
8		No	67.23	1.452 e+03	126.7
9		Yes	53.0835	3.3495e+03	127.9498
10	Activity:2	No	68.2	3.4495e+03	128.56
11		Yes	50.3966	7.1088e+03	145.0401
12		Yes	53.6969	1.0246e+05	145.0476
13		No	65.14	1.3246e+05	145.752
15		Yes	53.0835	4.2881e+04	127.9498
16		Yes	50.3966	7.0063e+04	145.0401
17		No	67.23	3.0063e+04	146.34
18		Yes	53.6969	1.0246e+05	145.0476
		Yes	48.8604	1.4563e+04	138.9498
1		Yes	54.5508	5.0267e+04	140.2728
2		Yes	56.7265	6.9477e+04	117.8600
3		Yes	51.1981	2.9540e+04	142.0947
4		Yes	56.7770	1.4857e+05	145.0673
5		Yes	46.4857	4.4852e+04	145.0401
6		Yes	51.5268	1.0205e+04	127.6884
7	Activity:3	Yes	54.5508	5.0267e+04	140.2728
8		Yes	56.7265	6.9477e+04	117.8600
9		Yes	51.1981	2.9540e+04	142.047
10		Yes	51.1981	2.95402e+04	142.0947
11		Yes	56.7770	1.4857e+05	145.0673
12		Yes	56.7770	1.4857e+05	145.0673
13		No	57.34	56.78	145.67
14		Yes	46.4857	4.4852e+04	145.0401
15		Yes	51.5268	1.0205e+04	127.6884
16		Yes	51.5268	1.0205e+04	127.6884

1		No	No	No	No
2		Yes	53.0643	3.3401e+04	121.2964
3		Yes	54.5508	1.3134e+04	129.5245
4		Yes	53.5156	3.1312e+04	142.1463
5		No	No	No	No
6		No	No	No	No
7		No	No	No	No
8		Yes	53.0643	3.3401e+04	121.2964
9	Activity:4	Yes	53.0643	3.3401e+04	121.2964
10		Yes	54.5508	1.3134e+04	129.5245
11		Yes	54.5508	1.3131e+04	129.5245
12		Yes	53.5156	3.1312e+04	142.1463
13		Yes	53.5156	3.1212e+04	142.1463
14		No	No	No	No
15		No	No	No	No
1	Activity:5	Yes	53.2740	1.4207e+04	133.0471
2		Yes	52.0412	3.5743e+04	120.9439
3		Yes	53.6249	4.1498e+04	120.8381
4		Yes	52.5063	4.0358e+04	128.1822
5		Yes	52.3400	3.9676e+04	127.7840
6		Yes	53.2740	1.4207e+04	133.0471
7		Yes	52.1431	1.4357e+04	132.1271
8		Yes	53.2740	1.4207e+04	133.0471
9		Yes	52.0412	3.5743e+04	120.9439
10		Yes	53.6249	4.1498e+04	120.8381
11		Yes	52.5063	4.0358e+04	128.1822
12		Yes	52.5063	4.0358e+04	128.1822

Table 3 Comparative analysis of proposed research work with existing work in terms of detection of different abnormalities and accuracy

Table 4. Performance analysis and comparison of proposed research work with existing works in terms of SNR, SSIM and PNSR.

Parameter	Existing work	Proposed work for Automated abnormality detection system
EEG signal coefficients bit size	8	8
Flip-flop used		6902
Delay		7.31ns
Area (Slices)		11093(9%)
Power utilized		0.088W
Slice registers		2872
No of LUT's		2871
Throughput		Size of the data/Delay=1.810Gbps
Latency		Product of Delay and size of data=4.419ns*8=35.352ns
Area-delay product		4.145*35.352ns =52380.365ns
Power and Delay product		0.082*12.637mW=14.653404mW/ns
Frequency	MHz	113.148MHz

8 Conclusion

HMM and SVM produced results in terms of sensitivity and accuracy, as shown in Tables 3 and 4. It can be observed from table.2 that the accuracy has been always higher than the sensitivity due to the availability of the number of training samples for every class. The convergence graphs also indicate that HMM requires a good number of iterations to train**.** Eventually, increasing the number of training samples can enhance performance. In addition that multi-resolution analysis involved in sampling the EEG at greater frequencies (> 1028Hz) proved to increase the detection of abnormality and might be used on EEG signals after FIR filter filtering. Average accuracy and detection rates have been considered since the models perform well in the detection of abnormality for the processed data sets, but it has been observed that when tested with individual EEG signals several errors have been produced in the form of false positive and false negative. The total EEG signals have been divided into windows of each 256 samples and processed through HMM and GMM. The proposed system exhibits a better outcome compared with other strategies like thresholding EEGs and combining ANNs with HMMs. Based on obtained results, a comparison has been made between proposed and previously published state-of-art works in the same area, it is found that 27% improvement in speed of process, 42% in identification of abnormalities in EEG signals and 35% improvement in accuracy.

References:

[1]. S. Bose, A. De and I. Chakrabarti, "Area-Delay-Power Efficient VLSI Architecture of FIR Filter for Processing Seismic Signal," in IEEE Transactions on Circuits and Systems II: Express Briefs, vol. 68, no. 11, pp. 3451-3455, Nov. 2021, doi: 10.1109/TCSII.2021.3081257.

[2]. E. G. Pale-Ramon, Y. S. Shmaliy, J. A. Andrade-Lucio and L. J. Morales-Mendoza, "Bias-Constrained H_2 Optimal Finite Impulse Response Filtering for Object Tracking Under Disturbances and Data Errors," in IEEE Transactions on Control Systems Technology, doi: 10.1109/TCST.2021.3118321.

[3]. X. Liu, M. Lewandowski and N. K. C. Nair, "A Morlet Wavelet-Based Two-Point FIR Filter Method for Phasor Estimation," in IEEE Transactions on Instrumentation and Measurement, vol. 70, pp. 1-10, 2021, Art no. 6503310, doi: 10.1109/TIM.2021.3075743.

[4]. X. X. Zheng, J. Yang, S. Y. Yang, W. Chen, L. Y. Huang and X. Y. Zhang, "Synthesis of Linear-Phase FIR Filters With a Complex Exponential Impulse Response," in IEEE Transactions on Signal Processing, vol. 69, pp. 6101-6115, 2021, doi: 10.1109/TSP.2021.3115352.

[5]. Y. S. Shmaliy, Y. Xu, J. A. Andrade-Lucio and O. Ibarra-Manzano, "Predictive Tracking Under Persistent Disturbances and Data Errors Using H_2 FIR Approach," in IEEE Transactions on Industrial Electronics, vol. 69, no. 6, pp. 6121-6129, June 2022, doi: 10.1109/TIE.2021.3087403.

[6]. S. M. J. A. Tabatabaee, M. Rajabzadeh and M. Towliat, "A Novel Low-Complexity GFDM Relay Communication System: Relay Selection and Filter-and-Forward," in IEEE Transactions on Signal Processing, vol. 69, pp. 5147-5158, 2021, doi: 10.1109/TSP.2021.3108679.

[7]. X. Liu, M. Lewandowski and N. K. C. Nair, "Erratum to “A Morlet Wavelet-Based Two-Point FIR Filter Method for Phasor Estimation”," in IEEE Transactions on Instrumentation and Measurement, vol. 71, pp. 1-1, 2022, Art no. 9900201, doi: 10.1109/TIM.2021.3127767.

[8]. Y. -E. Lee, N. -S. Kwak and S. -W. Lee, "A Real-Time Movement Artifact Removal Method for Ambulatory Brain-Computer Interfaces," in IEEE Transactions on Neural Systems and Rehabilitation Engineering, vol. 28, no. 12, pp. 2660-2670, Dec. 2020, doi: 10.1109/TNSRE.2020.3040264.

[9]. N. Richer, R. J. Downey, W. D. Hairston, D. P. Ferris and A. D. Nordin, "Motion and Muscle Artifact Removal Validation Using an Electrical Head Phantom, Robotic Motion Platform, and Dual Layer Mobile EEG," in IEEE Transactions on Neural Systems and Rehabilitation Engineering, vol. 28, no. 8, pp. 1825-1835, Aug. 2020, doi: 10.1109/TNSRE.2020.3000971.

[10]. M. Dora and D. Holcman, "Adaptive Single-Channel EEG Artifact Removal With Applications to Clinical Monitoring," in IEEE Transactions on Neural Systems and Rehabilitation Engineering, vol. 30, pp. 286-295, 2022, doi: 10.1109/TNSRE.2022.3147072.

[11]. S. Zahan, "Removing EOG artifacts from EEG signal using noise-assisted multivariate empirical mode decomposition," 2016 2nd International Conference on Electrical,

Computer & Telecommunication Engineering (ICECTE), 2016, pp. 1-5, doi: 10.1109/ICECTE.2016.7879634.

[12]. J. -S. Kang, S. Kavuri and M. Lee, "Adaptive EEG noise filtering for coherence analysis," 2014 International Winter Workshop on Brain-Computer Interface (BCI), 2014, pp. 1-4, doi: 10.1109/iww-BCI.2014.6782569.

[13]. C. Chou, T. Chen and W. Fang, "FPGA implementation of EEG system-on-chip with automatic artifacts removal based on BSS-CCA method," 2016 IEEE Biomedical Circuits and Systems Conference (BioCAS), 2016, pp. 224-227, doi: 10.1109/BioCAS.2016.7833772.

[14]. S. Siuly et al., "A New Framework for Automatic Detection of Patients With Mild Cognitive Impairment Using Resting-State EEG Signals," in IEEE Transactions on Neural Systems and Rehabilitation Engineering, vol. 28, no. 9, pp. 1966-1976, Sept. 2020, doi: 10.1109/TNSRE.2020.3013429.

[15]. Daqrouq, K.; Ajour, M.; Al-Qawasmi, A.R.; Alkhateeb, A. *"The discrete wavelet transform based electrocardiographic baseline wander reduction method for better signal diagnosis*",. J. Med. Imag. Health Inf.2018, 8, 1590–1597.

[16]. Lee, J.S.; Heo, J.; Lee, W.K.; Lim, Y.G.; Kim, Y.H.; Park, K.S. *"Flexible capacitive electrodes for minimizing motion artifacts in ambulatory electroencephalogram s"*. Sensors 2014, 14, 14732–14743

[17]. Yin, C.; Zhou, H.; Li, J. Facile *"one-step hydrothermal synthesis of PEDOT: PSS/MnO2 nanorod hybrids for high-rate supercapacitor electrode materials",*. Ionics 2019, 25, 685–695

[18]. Michael R Gold et al. *"The effect of TDAB duration and morphology on cardiac resynchronization therapy outcomes in mild heart failure: results from the resynchronization reverses Remodeling in Systolic left ventricular dysfunction (REVERSE) Study",* Circulation, page 112, 2012

[19]. Mei, Y.; Tan, G.Z.; Liu, Z.T.; Wu, H. *"Chaotic time series prediction based on brain emotional learning model and self-adaptive genetic algorithm"*. Acta Phys. Sin. 2018

[20]. He, S.; Sun, K.; Wang, R. *"Fractional fuzzy entropy algorithm and the complexity analysis for nonlinear time series"*. Eur. Phys. J.-Spec. Top. 2018, 227, 943–957.

[21]. Hashim, F.R.; Adnan, J.; Daud, N.G.N.; Mokhtar, A.S.N.; Rashidi, A.F.; Rizman, Z.I., *"Electroencephalogram noise cancellation using wavelet transform.*", J. Fundam. Appl. Sci. 2017, 9, 131–140

[22]. Feng, D.S.; Yang, D.X.; Wang, X. *"Ground penetrating radar numerical simulation with interpolating wavelet scales method and research on fourth-order Runge-Kutta auxiliary differential equation perfectly matched layer*", Acta Phys. Sin. 2016, 65, 23.

[23]. Karnewar, J.S.; Shandilya, D.V.K.; Tambakhe, M.D. *"A study on EEG signal analysis and EEG databases"*. Int. J. Res. Advent Technol. 2019, 7, 188–195

[24]. Tychkov, A.; Alimuradov, A.; Churakov, P. *"The emperical mode decomposition for EEG signal preprocessing"*. In Proceedings of the 2019 3rd School *on Dynamics of Complex Networks and their Application in Intellectual Robotics, DCNAIR"*, Innopolis, Russia, 9–11 December 2019

[25]. K. Kalimeri and C. Saitis, "Exploring multimodal biosignal features for stress detection during indoor mobility," in Proceedings of the 18th ACM International Conference on Multimodal Interaction, ICMI 2016, pp. 53–60, Japan, November 2016

[26]. Srinivasa Murthy et.al, "FPGA Implementation of high speed-low energy RNS based Reconfigurable-FIR Filter for Cognitive Radio Applications", WSEAS TRANSACTIONS on SYSTEMS and CONTROLDOI: 10.37394/23203.2021.16.24, E-ISSN: 2224-2856, Volume 16, 2021.